

## A sequence-based method for dynamic reliability assessment of MPD systems

Zhu, Jingyu; Chen, Guoming; Khan, Faisal; Yang, Ming; Li, Xinhong; Meng, Xiangkun; He, Rui

**DOI**

[10.1016/j.psep.2020.12.015](https://doi.org/10.1016/j.psep.2020.12.015)

**Publication date**

2021

**Document Version**

Final published version

**Published in**

Process Safety and Environmental Protection

**Citation (APA)**

Zhu, J., Chen, G., Khan, F., Yang, M., Li, X., Meng, X., & He, R. (2021). A sequence-based method for dynamic reliability assessment of MPD systems. *Process Safety and Environmental Protection*, 146, 927-942. <https://doi.org/10.1016/j.psep.2020.12.015>

**Important note**

To cite this publication, please use the final published version (if applicable). Please check the document version above.

**Copyright**

Other than for strictly personal use, it is not permitted to download, forward or distribute the text or part of it, without the consent of the author(s) and/or copyright holder(s), unless the work is under an open content license such as Creative Commons.

**Takedown policy**

Please contact us and provide details if you believe this document breaches copyrights. We will remove access to the work immediately and investigate your claim.

***Green Open Access added to TU Delft Institutional Repository***

***'You share, we take care!' - Taverne project***

**<https://www.openaccess.nl/en/you-share-we-take-care>**

Otherwise as indicated in the copyright section: the publisher is the copyright holder of this work and the author uses the Dutch legislation to make this work public.



## A sequence-based method for dynamic reliability assessment of MPD systems



Jingyu Zhu<sup>a</sup>, Guoming Chen<sup>a,\*</sup>, Faisal Khan<sup>b</sup>, Ming Yang<sup>c</sup>, Xinhong Li<sup>d</sup>, Xiangkun Meng<sup>e</sup>, Rui He<sup>a</sup>

<sup>a</sup> Centre for Offshore Engineering and Safety Technology, China University of Petroleum, Qingdao, Shandong 266580, China

<sup>b</sup> Centre for Risk, Integrity and Safety Engineering (C-RISE), Memorial University, St John's, NL, A1B 3X5, Canada

<sup>c</sup> Safety and Security Science Group, Faculty of Technology, Policy, and Management, Delft University of Technology, the Netherlands

<sup>d</sup> School of Resources Engineering, Xi'an University of Architecture and Technology, No.13 Yanta Road, Xi'an, 710055, China

<sup>e</sup> Navigation College, Dalian Maritime University, No. 1, Linghai Road, Dalian, China

### ARTICLE INFO

#### Article history:

Received 16 July 2020

Received in revised form 2 November 2020

Accepted 10 December 2020

Available online 15 December 2020

#### Keywords:

Reliability assessment

MPD system

GO-FLOW method

Dynamic bayesian network

Deepwater drilling

### ABSTRACT

Managed Pressure Drilling (MPD) system is widely used in the deepwater drilling operation. Reliability assessment plays a critical role in the MPD system in the management of drilling operation risk and the prevention of blowouts. However, the reliability assessment of the MPD system is challenged due to its sequential operations and multiple processes. Consequently, the present work proposes a sequence-based dynamic reliability assessment method, which focuses on the dynamic modeling of sequential operations for the MPD system by integrating GO-FLOW and dynamic Bayesian Network (DBN). GO-FLOW models are firstly used to define the time interaction between multiple phases for complex systems. A sequence-based mapping method is also proposed for the DBN to construct the reliability model of the MPD system throughout the entire drilling cycle. In the end, the case study analyzed by the proposed framework indicates that the reliability of the MPD system decreases with increasing drilling depth, and the reliability of “tripping in” is highest among four different phases, while the “drilling process” is the lowest. The method provides an important technique that can be implemented with online condition monitoring tools to assess and monitor the reliability of the MPD operation in real-time.

© 2020 Published by Elsevier B.V. on behalf of Institution of Chemical Engineers.

## 1. Introduction

Deepwater drilling operation faces not only the harsh environment but the operational challenges of complex operations and equipment (Abimbola et al., 2014; Pui et al., 2017; Sule et al., 2018). Unintended influxes, kicks, and blowouts may occur when complex geological environments are encountered during drilling operations with a narrow drilling window (Wu et al., 2019). The MPD system has been widely developed to overcome the challenge of well control due to its precise control over wellbore pressures (Hannegan, 2006). Meanwhile, additional equipment also increases the complexity and high risk of the MPD operations compared with the conventional drilling operation. The reliability assessment of the MPD system should be further investigated to prevent kicks or blowout in deepwater drilling.

In the past decades, various methods have been explored to assess system reliability, including fault tree analysis (FTA), failure mode and effects analysis (FMEA), Markov approach, Monte Carlo (MC), GO methodology and GO-FLOW method, etc. FTA and FMEA are two of the earliest widely used reliability analysis methods (Jia and Lin, 2015). However, both of them are not capable of the reliability analysis of complex systems with dependent relationships (Xu et al., 2002). The Markov approach is applied to reliability evaluation for redundant and non-redundant systems with substantial flexibility (Kim et al., 2005). Nevertheless, this method may suffer state-explosion consequences when applied to a large-scale system (Veeramany and Pandey, 2011). The GO methodology is a success-oriented analysis method of system reliability, which was initially developed by Kaman Sciences Corporation to assess the complex system (Shen et al., 2003; Liu et al., 2018). The GO-FLOW method was developed based on GO methodology to actualize reliability analysis for complex systems with a phased mission problem. By considering common cause failure analysis and logic loop solution, the GO-FLOW method was improved and further applied to elevator systems, railway systems, and nuclear power plant sys-

\* Corresponding author.

E-mail address: [offshore@126.com](mailto:offshore@126.com) (G. Chen).

tems (Matsuoka and Kobayashi, 1988,1989, 1997; Hashim et al., 2013, 2014; Yang et al., 2014; Liu et al., 2016). Based on the GO-FLOW technique, Hashim et al. conducted a reliability evaluation for AP1000 ADS system to determine the influencing factors (Hashim et al., 2014). To assess reliability in real-time, a risk monitoring system was developed based on the GO-FLOW method with online received information (Yang et al., 2014). In addition, Yang et al. presented a new framework of an improved risk monitor system based on the GO-FLOW technique, which integrated multiple applications of the investigation of risk factors, risk monitoring, and management (Yang et al., 2020). The method has also been applied to an auxiliary feedwater system, aircraft electro-hydrostatic actuator, chemical and volume control system, etc. (Liu et al., 2016; Lan et al., 2017; Lu et al., 2019). Although the GO-FLOW method has been applied to the reliability assessment of many systems, some limitations still exist. There are many GO-FLOW operators, which induces the calculation process intricate. Besides, GO-FLOW cannot construct intermittent operation charts, especially for the entire drilling cycle of a sophisticated MPD system (Yang et al., 2014).

Bayesian Networks (BNs) are directed acyclic graphs comprised of nodes and arcs that represent a set of variables and their conditional dependencies (Pearl, 1988). The application of dynamic Bayesian Network (DBN) for conducting reliability evaluation and quantitative risk analysis is relatively new and has become very popular recently (Khakzad et al., 2013a; Bhandari et al., 2015; Amin et al., 2018). Considering the dynamic variations of the complex system, classical BN has been extended to model systems in the dynamic domain, so the DBN was developed (Murphy, 2002). This method possesses the features of updating new evidence and posterior reasoning and can also overcome the limitation of uncertain knowledge (He et al., 2018). As an effective method for the reliability or risk analysis, it was widely applied to the offshore oil and gas industry and other fields specific including deepwater drilling operations (Bhandari et al., 2015; Khakzad et al., 2013b; Chang et al., 2019), leakage failure of submarine pipelines (Li et al., 2016, 2019), fire alarm systems (Amin et al., 2018), catastrophic shipping accidents (Zhang and Thai, 2016), and collision hazards for the High Speed Craft (Trucco et al., 2008). For the MPD system in deepwater drilling, the risk of deepwater drilling operations was evaluated by BN method (Abimbola et al., 2015). Furthermore, the reliability assessments of kicks control operation of the MPD system were performed by using the FTA and BN methods (Sule et al., 2018). However, most of the previous studies rarely took account of different drilling phases and the sequence between different drilling phases in the MPD drilling process.

The drilling operation of the MPD system is a complicated task, which faces operational sequences, phased mission problems, and multiple processes. For instance, the MPD system includes the phased missions of drilling and making connection, and drilling contains multiple processes of rig pump action and drilling string open, which are all subjected to a specific time sequence. The appointed time sequence is critical for the reliability assessment of such an intermittent system. The GO-FLOW method is applicable to systems with complex sequences of system operation or system state changes over time (Matsuoka and Kobayashi, 1988,1989). On the other hand, DBN is a powerful and flexible tool to model dynamic system behavior and update reliability with life cycle data (Zhu and Collette, 2015; Wu et al., 2019). The drilling operation of the MPD system is a typical phased-mission process, facing time sequence problems (Zhang et al., 2018). One unique advantage of DBN is that it can be used to develop time sequence models of phased-mission systems since it contains a series of time slices and temporal links. In any drilling phases of the MPD system, its GO-FLOW models can be directly converted based on the function charts system structure. It relaxes the existing limitations of the model building of the DBN method. In addition, the DBN models of

the entire drilling cycle for the MPD systems can also be developed due to the ability to capture the dependency relationships among different phases. Therefore, GO-FLOW and DBN can be used for the reliability assessment of time sequences of MPD systems. Aiming to realize the dynamic sequence reliability of the MPD system, a novel method for dynamic reliability assessment of MPD operation is developed by integrating GO-FLOW with DBN. The potential contributions can be specified as (1) The primary novelty of proposed methods is the idea of dynamic sequential modeling for the reliability assessment of MPD systems. (2) GO-FLOW models are firstly used to define the interaction between multiple processes. (3) Since there is no specific semantic to guide the model development of DBN, a sequence-based mapping method is proposed to enrich the ways of developing DBN.

The rest of this paper is organized as follows. A brief discussion on the GO-FLOW method and DBN method is provided in Section 2. The method for the reliability assessment of the MPD system is proposed in Section 3. Applications of the method are presented by a case study in Section 4. Section 5 provides the reliability analysis and results of the MPD system in deepwater drilling. The conclusions of this paper are demonstrated in Section 6.

## 2. Basic methods

### 2.1. GO-FLOW method

GO-FLOW can evaluate an extensive system with complex operational sequences (Hashim et al., 2013, 2014). The GO-FLOW methodology is a success-oriented methodology for system reliability analysis. It includes two necessary steps: first, construct the GO-FLOW chart for the physical system, and then calculate the system reliability. (Matsuoka and Kobayashi, 1988, 1989, 1997). The system function diagram can be directly converted into a GO-FLOW modeling by graphical deduction. And then, the probability of occurrence of different states in the system is calculated by one computer run.

The classic GO-FLOW method utilizes 14 basic operators and signal lines to model the system function (Hashim et al., 2013; Fan et al., 2016). The meanings and symbols of 14 operators are shown in Fig. 1. According to their function, these operators can be divided into function operators, logical operators, and signal operators. Generally, the function operators are used to model the physical component and indicate the normal or failure condition of the component; the logical operators simulate the consistent relationship between system components, and the signal operators represent the external input signal of the system (Yang et al., 2014, 2020).

The signal lines are used to connect the inputs and outputs to the operators. A signal represents some physical quantity or information, such as fluid flow, electric currents, required signals, etc. A variable called 'intensity' is associated with a signal line. Usually, the intensity can describe the digital features and represent the probability of signal existence. If a signal is used as a sub-input signal to the type 35, 37, or 38 operators, the intensity represents a time interval between the successive time points (Liu et al., 2016).

When the GO-FLOW chart is constructed, a limited number of discrete-time points need to be defined to indicate the system operation sequence. The time points do not necessarily represent real-time but reflect an ordering of the system operation. The number of time points is defined by the analysts, which depends on the objective of the analysis and the sequence of the system running. Finally, these data are input to the GO-FLOW model, and the intensity of the final signal at all-time points is obtained.

The GO-FLOW method has the following advantages: (1) The GO-FLOW chart can be directly constructed according to the physi-

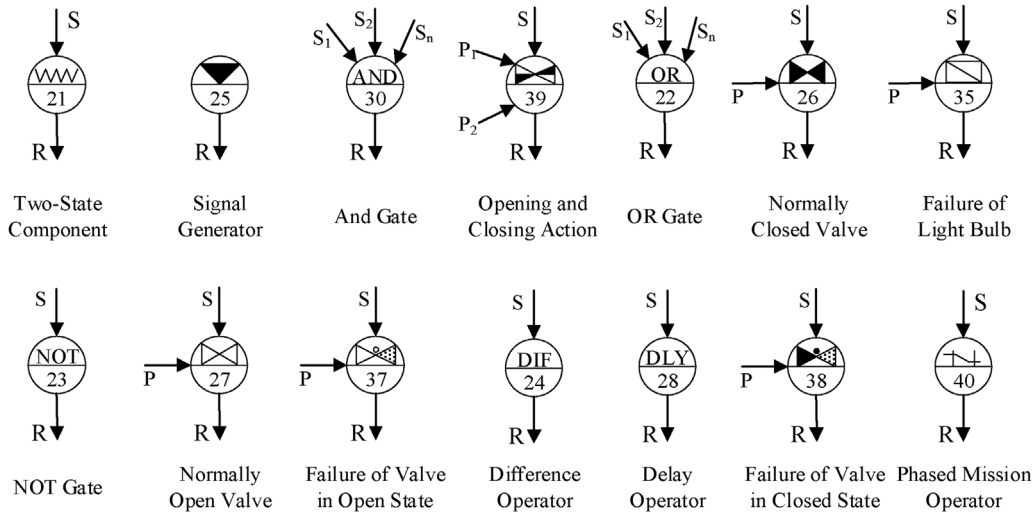


Fig. 1. Operators defined in the GO-FLOW method.

cal layout of the system; (2) Revisions and updates to the GO-FLOW charts are readily completed; (3) The GO-FLOW chart contains all possible system operational states. However, like other reliability assessment methods, GO-FLOW also has its defects. The problem of the combinatorial explosion becomes very significant as the number of components increases. Besides, GO-FLOW cannot construct hierarchical charts. Furthermore, GO-FLOW is unable to build intermittent operation charts for sophisticated systems.

2.2. Dynamic bayesian network method

Bayesian Network (BN) is a graphical technique, which has been applied to qualitative and quantitative risk analysis due to its forward analysis and backward analysis (He et al., 2018). A BN consists of nodes and arcs, in which the nodes represent states of variables, and arcs depict causal relationships between the linked nodes. The qualitative analysis can be performed by a network structure, while the quantitative calculation is expressed by assigning conditional probability distributions to the nodes. Considering the conditional dependencies between the variables, the joint probability distribution  $P(U)$  of variables  $U = \{X_1, X_2, \dots, X_n\}$  in the network can be written as (Bhandari et al., 2015):

$$P(U) = \prod_{i=1}^n P(X_i | Pa(X_i)), i = (1, 2, \dots, n) \tag{1}$$

Where  $Pa(X_i)$  is the parent set of any node  $X_i$ .

BN takes advantage of Bayes theorem to update the prior occurrence (or failure) probability with new observations of evidence  $E$ . The updating posteriors of  $P(U)$  could be obtained from Eq. (2) (Khakzad et al., 2013b).

$$P(U|E) = \frac{P(U, E)}{P(E)} = \frac{P(U, E)}{\sum_U P(U, E)} \tag{2}$$

A dynamic Bayesian Network (DBN) consists of a sequence of time slices and temporal links developed from the conventional static BN (He et al., 2018). In other words, the time attribute is added to the static BN, and the trend of the variables and their causal relationship can be presented in various time slices at different time points. Fig. 2 shows a simple DBN model with three nodes. ( $X_1, X_2$ ) are the parent node of  $Z$  in initial time  $t_1$  under phase 1. According to the time series, the DBN structure expanded to  $t_{n-1}$  and  $t_n$

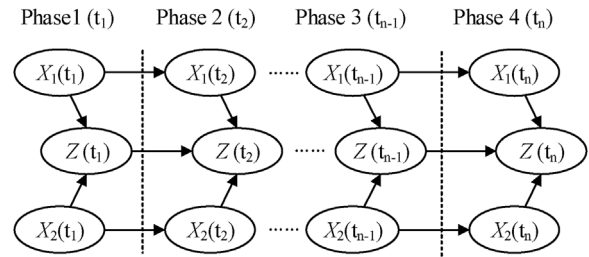


Fig. 2. A simple DBN model.

under different stages. Meanwhile, the dynamic characteristics and reliability of the target system can be captured (Amin et al., 2018).

Compared to static BN, the joint probability distribution function of a DBN for time  $t = 1$  to  $N$  can be expressed as (Li et al., 2016):

$$P(Z_{1:N}) = \prod_{t=1}^N \prod_{i=1}^n P(Z_{i,t} | Pa(Z_{i,t})) \tag{3}$$

Where  $Z_{i,t}$  is the  $i$ th node at time  $t$ ;  $Pa(Z_{i,t})$  is the parent set of any node  $Z_{i,t}$ ;  $n$  is the number of nodes;  $N$  is the number of time points in the network.

Model development and parameter estimation are two critical parts for reliability assessment by using the DBN method. However, a weak point of DBN is that there is no specific semantic to guide model development. To overcome this problem, many studies try to translate classical dependability models such as FT, event tree, and Markov model into BN models (Liu et al., 2018). But this way has no application to sequential operation systems, especially for the complex operations of the MPD system.

3. Proposed method for MPD system

3.1. Description of the MPD system

Generally, the MPD operation comprises several sub-operations or phases, i.e., drilling ahead, making a connection, tripping, casing and cementing (Arild et al., 2009). The MPD system is different from conventional drilling practices, which rely on mud weight, shutting in the BOP, and circulating out influx to avoid the kicks and blowouts (Sule et al., 2018; Quoc et al., 2016). The MPD system can process certain influxes by utilizing the Rotating Control

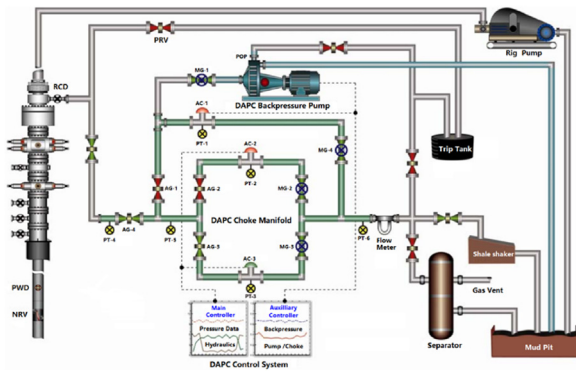


Fig. 3. Dynamic annular pressure control of the MPD process flow diagram.

Device (RCD) bearing assembly and the Choke Manifold without activating secondary safety barriers (Gabaldon et al., 2014; Abimbola et al., 2015). International Association of Drilling Contractors (IADC) defined that MPD is an adaptive drilling process employed to control the annular pressure profile throughout the wellbore (Hannegan, 2006). The pressure margins are usually narrow in deepwater drilling due to its complex conditions and exact requirements (Wang et al., 2011). MPD technology is a relatively advanced method for pressure control during the drilling operation. This technology aims to ascertain the downhole pressure environment limits and manage the annular hydraulic pressure profile accordingly. The equipment layout of the MPD system is shown in Fig. 3 (Chustz et al., 2008).

### 3.2. The combination of DBN and GO-FLOW

According to the GO-FLOW model of the target system, a DBN model is established based on mapping rules. First, the operator should be converted into a node of the Bayesian network, and the conditional probability table (CPT) of the mapping node needs to be given based on the mapping algorithm of each operator. As shown in Fig. 4, the frequently-used operators and the equivalent DBN nodes in the MPD system include type 25 of the signal operator, type 22, 23, 30 of logical operators, and type 21, 26, 35 of function operators. Besides, the different characters in DBN nodes represent different meanings. Hereinto,  $S$  represents the input signal,  $R$  represents the output signal,  $t$  represents time point, and  $t'$  is the time point before time  $t$ . The Type 21 operator usually describes some two-state physical equipment. The output signal will be presented when the input signal is given and the operator is good. Therefore, there is a character  $C$  for type 21 operator in the equivalent DBN model compared with the GO-FLOW method, and  $C$  represents the operator itself. Similarly, the character  $C$  for type 26 operator also represents the component itself, but it is unnecessary for other operators. Due to space limitations, the mapping rules of type 25, 22, 35 operators are introduced detailed in this paper, and the remaining operators can be computed based on the following methods.

#### (i) Signal operator-type 25

In the GO-FLOW method, the type 25 operator is dedicated to simulating a single-signal generator without input signals but with one output signal. This operator can generate one or some signals at one specific or some consecutive time points. The signal given by this operator is commonly used to start the component. The output signal of the type 25 operator has two states: success and failure. The success state means the signal can be sent out successfully. Taking the conditional statement of time point  $t_1$  as an example,

the intensity  $R(t_1)$  represents the probability of the signal being emitted at time point  $t_1$ . Instead, the failure state means there are no signal outputs, and the failure probability also can be calculated by  $1-R(t_1)$ . Therefore, the BN model of type 25 operator is shown in Fig. 4(d), and its CPTs can be defined in Table 1, where  $t_i$  represents conditional statement at different time points.

#### (ii) Logical operator-type 22

There are three logical operators in the GO-FLOW method, including types 22, 23, and 30 operators, which correspond to the “OR” gate, “NOT” gate, and “AND” gate. For simplicity, this section takes the “OR” gate as an example to describe the mapping rules of logical operators. The type 22 operator has more than one input signal ( $S_j$ ) but only one output signal  $R(t)$ . According to the definition of the “OR” gate, the output signal  $R$  is in the failure state when all the input signals break down. Assuming that there are three input signals, the output intensity can be obtained by Eq. (4). The equivalent DBN model of the “OR” gate operator with three input components ( $S_1, S_2, S_3$ ) is shown in Fig. 4(b). Based on the logical relationships of three input signals, the CPTs of type 22 operator can be defined in Table 2. Just as the general input signal, each input signal of type 22 operator also has two states: success and failure. Taking the input signal  $S_1$  as an example, the success state means that the input signal  $S_1$  exists, while it is the opposite of the failure state. The corresponding CPTs are shown in Table 3. Herein,  $P(t_i)$  represents the failure probability of input signal  $S_1$  at time point  $t_i$ .

$$R(t) = 1 - [(1 - S_1(t)) \cdot (1 - S_2(t)) \cdot (1 - S_3(t))] \quad (4)$$

#### (iii) Function operator-type 35

Type 35 operator is used to emulate a component (e.g., a rig pump) with increasing failure probabilities as the increasing working time in the MPD system. It has the primary input signal  $S(t)$ , several sub-input signals  $P(t)$ , and one output signal  $R(t)$ . The primary input signal  $S(t)$  can be obtained from the previous operator. The intensity of the sub-input signal denotes a time interval in which the failure probability of the component gradually increases due to the failure rate  $\lambda$ . Generally, assuming that  $\lambda$  is a constant and the failure probability of this component follows an exponential distribution, which can be calculated from Eq. (5). For MPD systems, the rig pump or some physical equipment has two states: success and failure. Therefore, the  $P(t)$  can be used to indicate the probability of the failure state of a component. The input signal also has two states: success and failure (existence and non-existence). The output signal  $R$  is in the success state when the input signal  $S$  and sub-input signal  $P$  are both in success. The DBN model of type 35 operator is shown in Fig. 4(g), and the CPTs of this operator can be defined in Table 4. Similar to input signal  $S_1$ , the CPTs of  $P$  and  $S$  can also be determined in Table 5.

$$P(t) = \int_0^t \lambda e^{-\lambda t} dt \quad (5)$$

### 3.3. Integrated framework

The MPD system requires high reliability and should always be functional. When the MPD system fails, some undesired consequences may occur, e.g., kicks, blowout, equipment damages, casualties, and environmental disruptions. An integrated framework to assess the dynamic sequence reliability is proposed to overcome sequential operations and phased mission problems. The framework of the proposed method is shown in Fig. 5. The proposed method concludes five steps:

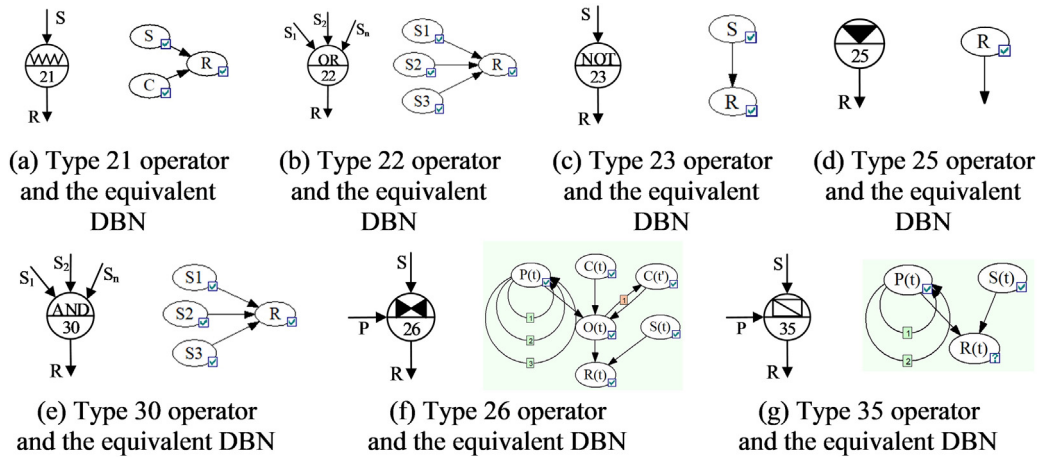


Fig. 4. Operators in GO-FLOW model and the corresponding DBN model.

**Table 1**  
CPTs of type 25 operator.

Time	$t_1$		$t_i$		...	$t_n$	
State	success	failure	success	failure		success	failure
Value	$R(t_1)$	$1-R(t_1)$	$R(t_i)$	$1-R(t_i)$		$R(t_n)$	$1-R(t_n)$

**Table 2**  
CPTs of type 22 operator.

$S_1$	success				failure			
$S_2$	success				failure			
$S_3$	success	failure	success	failure	success	failure	success	failure
$R$	success	1	1	1	1	1	1	0
	failure	0	0	0	0	0	0	1

**Table 3**  
CPTs of input signal  $S_1$ .

Time	$t_1$		$t_i$		...	$t_n$	
State	success	failure	success	failure		success	failure
Value	$1-P(t_1)$	$P(t_1)$	$1-P(t_i)$	$P(t_i)$		$1-P(t_n)$	$P(t_n)$

**Table 4**  
CPTs of type 35 operator.

$P$	success				failure			
$S$	success				failure			
$R$	success	1	0	0	0	0	0	0
	failure	0	1	1	1	1	1	1

**Step 1:** Define the system and collect the necessary information. The scope of the MPD system is defined firstly and studied adequately. Meanwhile, the required information, including the system function, structural composition, operation principle, failure data of equipment, well structure, operation schedule, etc. need to be collected in the whole drilling operation. These may help to

understand the layout of the MPD system, process techniques, and equipment functions.

**Step 2:** Construct GO-FLOW models for different drilling phases. The MPD drilling operation is divided into four phases based on Section 2.2. Success criteria are determined considering their functions and objectives for different drilling phases, and flowcharts are

**Table 5**  
CPTs of  $P$  and  $S$ .

Time	$t_1$		$t_i$		...	$t_n$	
State	success	failure	success	failure		success	failure
$P$	$1-P(t_1)$	$P(t_1)$	$1-P(t_i)$	$P(t_i)$		$1-P(t_n)$	$P(t_n)$
$S$	$1-S(t_1)$	$S(t_1)$	$1-S(t_i)$	$S(t_i)$		$1-S(t_n)$	$S(t_n)$

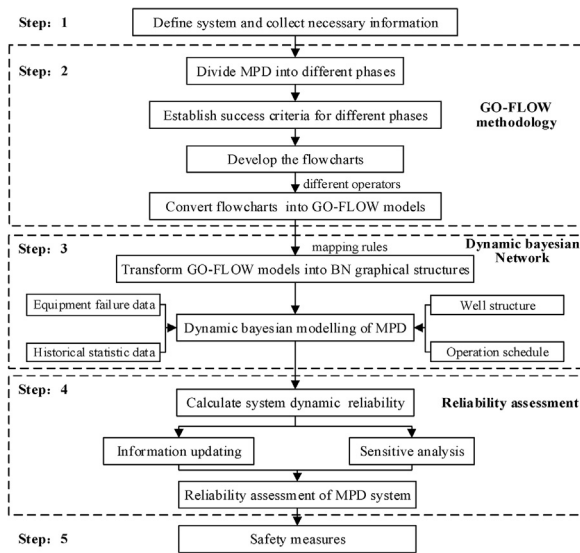


Fig. 5. The framework of reliability assessment for the MPD system.

developed correspondingly. Hereinto, the success criteria refer to the purposes of different phases. For the drilling process, it means that the step of separate muds achieved without a kick event. Different flowcharts can be converted into GO-FLOW models by using signal lines and operators. The GO-FLOW models represent different functions of the system during the drilling operation.

**Step 3:** Establish the DBN model for the MPD operation. Four different DBN models can be transformed from GO-FLOW models based on the mapping rules in Section 3.3.2. The DBN model is established based on the selected well structure and operation schedule. The failure probabilities of equipment and operations are obtained from OREDA database (OREDA, 2002), published literature, expert knowledge, or historical statistic under specific industries (Khakzad et al., 2013a). Moreover, the drilling operation of the MPD system is continuous. The DBN models of the entire drilling cycle should be constructed according to the well depths.

**Step 4:** Assess the reliability of the MPD system. In this step, system reliability can be calculated by DBN modeling during the drilling cycle. Reliability analysis includes two parts, i.e., sensitive analysis and information updating. Sensitivity analysis is carried out to identify the critical components and rank the importance of system components. Information updating aims to update the real-time reliability once some new evidence is collected.

**Step 5:** Safety measures. Identifying critical components and units for the operating systems can be performed with sensitivity analysis and information updating. To improve the reliability of the MPD system, safety measures and an efficient maintenance plan can be proposed based on the assessment results.

4. Case study

4.1. Different MPD drilling phases and corresponding flow charts

MPD technology includes four different phases: drilling process, making a connection, tripping out, and tripping in, as shown in Fig. 6. It is necessary to start the rig pump for the drilling process when carrying out one particular hole section operation. And then, the wellhead pressure should be increased to make a connection after stopping the rig pump. Drilling to a certain depth, after the drilling process and making a connection cycling alternately, the drill tools need to be replaced by the tripping out operation. The drilling tools should be combined and tripped in for the next section of drilling. The corresponding operating procedures will be initiated to control the BHP during the drilling operation.

In this section, a case study of the MPD system in the South China Sea is conducted to verify the effectiveness of the proposed method. Generally, the drilling process of the MPD system includes four well sections, which are 26", 17–1/2", 12–1/4" and 8–1/2" well sections. As mentioned in Section 2.2, there are four different drilling phases in each well section, and the phases of the drilling process and making a connection are alternated during each well section. The drill tools need to be replaced in the 'tripping out' phase at the end of the prior well section. And then, the drilling tools will be combined again and tripped in the next well section. The phases of the drilling process and making a connection are alternated until the well completion, as shown in Fig. 6. The drilling phases of the MPD system are introduced detailedly and corresponding flowcharts are constructed thoroughly, as shown in Fig. 7.

- (i) Drilling process. Mud density should be determined based on formation parameters before the drilling fluid is pumped into the bottom hole via drilling strings. Traversing RCD, drilling fluid will return from the wellbore to choke manifolds, and the wellhead backpressure can be controlled by adjusting choke valves. There are three flow lines for choke manifolds. The flow lines 1 installed the choke valve AC-2, which is mainline for returned drilling fluid. If flow line 1 fails, the flow line 2 installed the choke valve AC-3 begins to take effect. The back-flow line 3 and the pressure relief valve will work to convey the fluids and choke manifolds against overpressure hazards

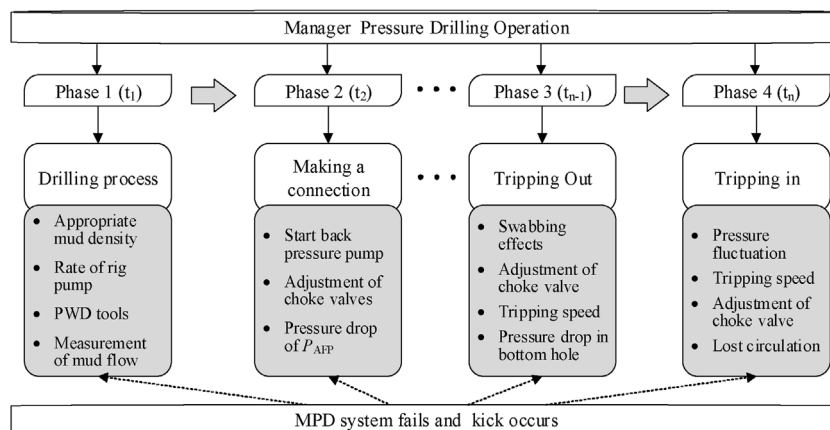


Fig. 6. The managed pressure drilling phases.



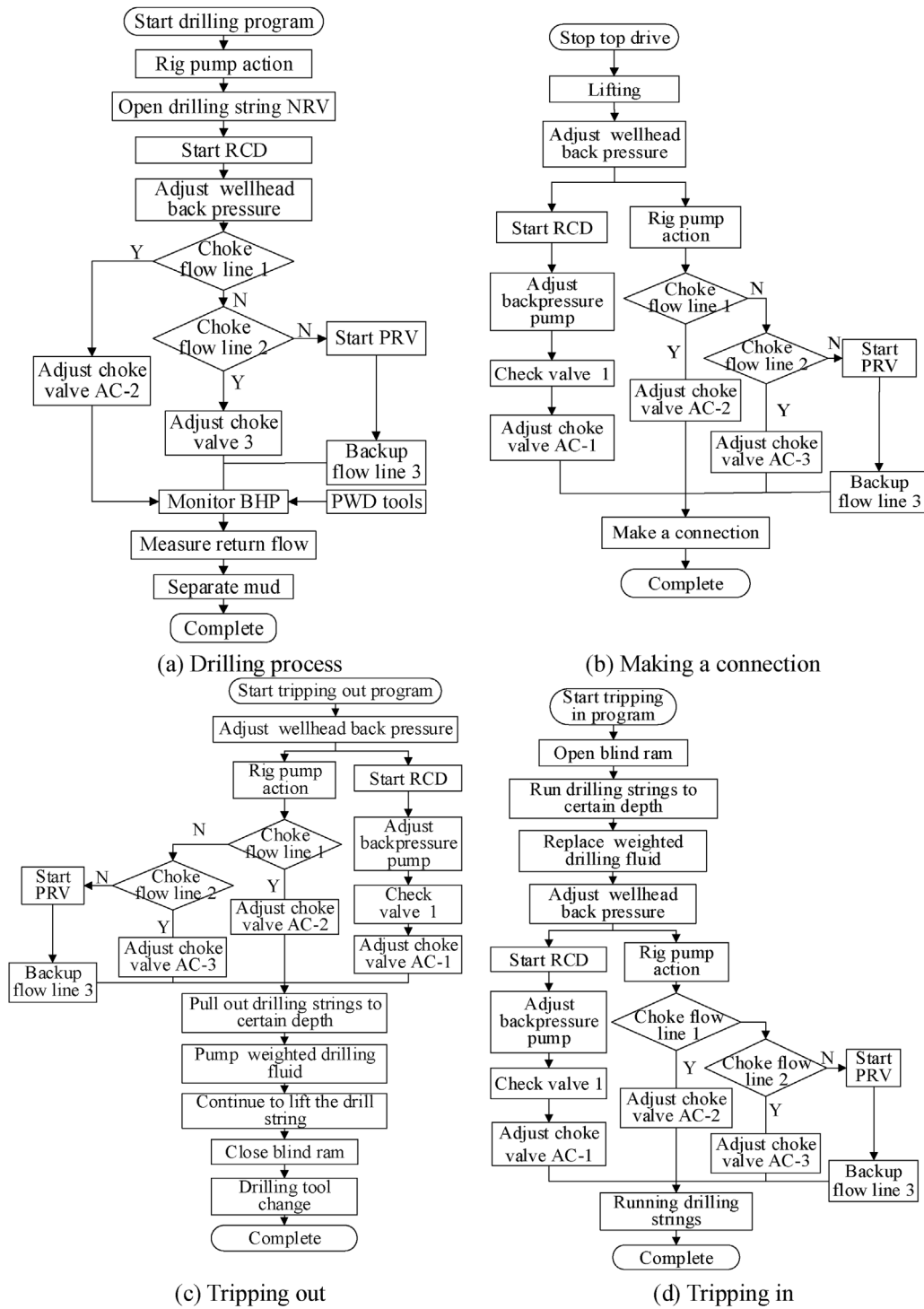


Fig. 7. Flow charts of the MPD system during the entire drilling cycle.

when both flow line 1 and flow line 2 fail. Flow measurement is carried out when effusive fluid passes through the Coriolis flowmeter. Finally, the BHP can be monitored all the time during the drilling process. If there is no abnormality in BHP, the fluid will flow into the mud pool via the shale shaker. Returned fluids can be separated into gas, oil, and contamination-free drilling fluid by a separator if this process succeeds. The flow chart of the drilling process is constructed, as illustrated in Fig. 7(a).

(ii) (Make a connection. The flow chart of making a connection is shown in Fig. 7(b). The PAFP gradually decreases to zero with the pump off and stop circulating when the operation of making a connection functions. To ensure that the BHP is always slightly higher than the formation pressure, the backpressure pump needs to be started, and the wellhead backpressure will increase slowly to compensate for the pressure drop of PAFP. Nevertheless, the operation of ‘pump on’ is the opposite of the ‘pump off’.

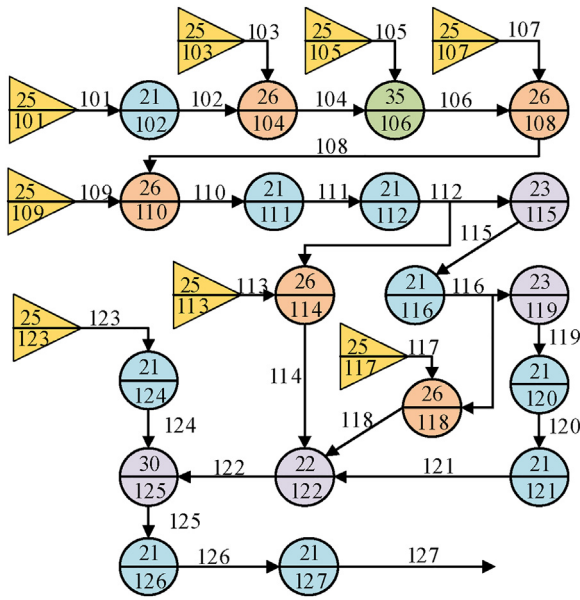


Fig. 8. GO-FLOW model of drilling process for the MPD system.

- (iii) Tripping out. The drilling strings are lifted to the projected depth by injecting the heavy mud cap, and the tripping speed needs to be controlled strictly in this phase. There is an excessive pressure drop in the bottom hole due to the swabbing effects and stopping downhole circulation. Hence, the speed of the backpressure pump and the choke valve opening of manifolds should be regulated in time. The rest of the drill strings are lifted to the derrick floor in the usual way. Similarly, the corresponding flow chart of tripping out is shown in Fig. 7(c).
- (iv) Tripping in. Before the operation of tripping in, bottom hole assembly may be lowered to the casing shoe and drilling circulating also be started by rig pumps. Choke manifolds and DAPC systems can be used to avoid lost circulation. Meanwhile, the tripping speed should be kept in reasonable bounds, and then the heavy mud cap will be displaced. The drilling bits are run into the bottom to prepare for the next hole section. And the flow chart of tripping in is constructed in Fig. 7(d).

4.2. Convert flow charts into GO-FLOW model

As shown in Fig. 8, the GO-FLOW model of the MPD drilling process is converted from its flow chart based on the function and structure of the system. Based on the operation sequence and the

Table 6  
The operator parameters of the drilling process for the MPD system.

Operator No	Type	Meaning	Parameter	Operator No	Type	Meaning	Parameter
101	25	Initial time	$R(1) = 0, R(t) = 1 (t \neq 1)$	115	23	Not gate	/
102	21	Start signal of drilling	$P = 1.0 \times 10^{-4}$	116	21	Choke flow line 2	$P = 3.6 \times 10^{-4}$
103	25	Start signal of rig pump	$R(2) = 1, R(t) = 0 (t \neq 2)$	117	25	Start signal of choke valve 3	$R(t) = 0, t \neq (4,5) R(t) = 1, t=(4,5)$
104	26	Rig pump	$P_p = 4.3 \times 10^{-5} P_g = 4.3 \times 10^{-4}$	118	26	Choke valve 3	$P_p = 2.5 \times 10^{-4} P_g = 2.5 \times 10^{-3}$
105	25	Time interval	$t = 3.75 \text{ h}$	119	23	Not gate	/
106	35	Failure rate of rig pump	$\lambda = 2.52 \times 10^{-6} \text{ h}^{-1}$	120	21	PRV	$P = 2.2 \times 10^{-5}$
107	25	Start signal of DS-NRV	$R(3) = 1, R(t) = 0 (t \neq 3)$	121	21	Backup flow line 3	$P = 3.6 \times 10^{-4}$
108	26	DS-NRV	$P_p = 1.3 \times 10^{-6} P_g = 1.3 \times 10^{-5}$	122	22	OR gate	/
109	25	Start signal of RCD	$R(3) = 1, R(t) = 0 (t \neq 3)$	123	25	Start signal of measurement	$R(t) = 0, t \neq (4,5) R(t) = 1, t=(4,5)$
110	26	RCD	$P_p = 6.7 \times 10^{-6} P_g = 6.7 \times 10^{-5}$	124	21	PWD tools	$P = 1.1 \times 10^{-5}$
111	21	Adjust wellhead back pressure	$P = 1.0 \times 10^{-4}$	125	30	AND gate	/
112	21	Choke flow line 1	$P = 3.6 \times 10^{-4}$	126	21	Flow measurement	$P = 1.1 \times 10^{-5}$
113	25	Start signal of choke 2	$R(t) = 0, t \neq (4,5) R(t) = 1, t=(4,5)$	127	21	Mud Separator	$P = 2.0 \times 10^{-4}$
114	26	Choke valve 2	$P_p = 2.5 \times 10^{-4} P_g = 2.5 \times 10^{-3}$				

flow chart, the drilling process can be divided into five time points. Time point 1 is an initial time. At time point 2, the rig pump begins to operate. At time point 3, which is next to time point 2, drilling strings NRV and RCD are started. At time point 4, choke valve 2 and 3 begin to operate. Time point 5 is 0.1 h after time point 3 and the drilling operation of one thribble is completed. Similarly, other GO-FLOW models of the MPD drilling phases also can be established according to their flow charts, as shown in Appendix A.

As a critical element of the GO-FLOW model, different operators should be selected appropriately to represent their operations and components. In total, 27 operators are used in this GO-FLOW model, from the initial drilling signal of operator 101 to the complete signal of final operator 127. Herein, type 25 operators are used to generate input signals at five time points. The rig pump, drilling strings NRV, and RCD are denoted by type 26 operators. There are two critical parameters in which  $P_p$  represents the failure probability of start-up, and  $P_g$  represents the failure probability of the usual start. Given the rig pump may fail as the increasing service time, the rig pump can be presented by type 35 operators and the failure rate  $\lambda$  is a constant or variable. Flow lines, valves, flowmeter, and separator only have two statuses, which can be denoted by type 21 operators. The logical relationship can be presented by type 22, 23, and 30 operators. The operator parameters of the drilling process for the MPD system are given in Table 6, which are investigated from published literature, expert knowledge, or historical data statistics (Abimbola et al., 2014; Sule et al., 2018; Abimbola et al., 2015; Rathnayaka et al., 2013).

4.3. DBN graphical structure of different MPD drilling operation

To overcome the limitations of conventional reliability assessment methods (e.g. FTA or FMEA etc.), the equivalent DBN model (Fig. 9) is developed from the constructed GO-FLOW model of the drilling process for the MPD system. The CPTs can be determined according to the collected operator parameters. A distinct advantage of DBN is that the computational process is more convenient and user-friendly than GO-FLOW. Another advantage of DBN is that the dynamic system reliability can be obtained through observational evidence updating. In Appendix A, other DBN models of the MPD drilling phases also can be established according to their flow charts in the same way.

To evaluate the system reliability throughout the entire drilling cycle, reliability assessment should be implemented, which combines the drilling process, making a connection, tripping out, and tripping in phases. The specific parameters of well profile and work schedule are presented in Appendix B, which were obtained from a certain well in South China Sea. Given that the 36" conductor is jetted into shallow subsea soil, four remaining sections need

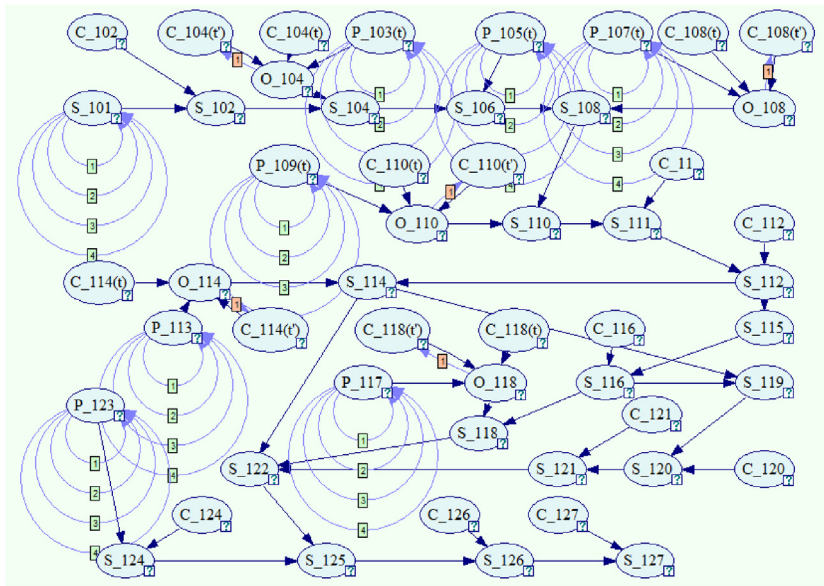


Fig. 9. DBN model of the drilling process for the MPD system.

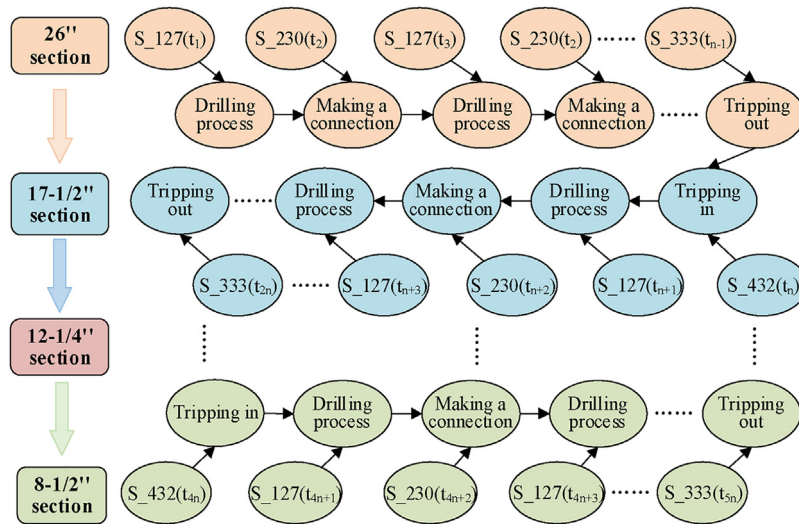


Fig. 10. DBN model of the entire drilling cycle for the MPD system.

to be drilled using the MPD system, which includes 26" section, 17–1/2" section, 12–1/4" section, and 8–1/2" section. The results of end nodes for different phases represent the reliability of the MPD operation in different drilling depths or time. The DBN model of the entire drilling cycle is established in Fig. 10.

**5. Results and discussion**

*5.1. Dynamic reliability assessment*

The output intensities of components in the drilling process for the MPD system are expressed in Fig. 11. Six components are selected to present a variety of intensities at different time points. All output intensities of components equal 0 at time point 1 because the system has not been started in the initial time. As the enabled operator, the intensity of S\_101 equal to 1 after time point 2. The sequential operation of operator S\_106 is similar to operator S\_101. However, output intensities begin to decrease with traversing a series of components. Although the operator S\_111 and S\_112 start at time point 3 simultaneously, the output intensity of operator

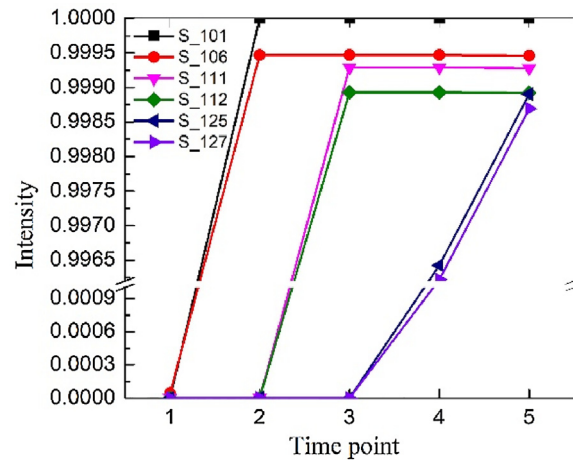


Fig. 11. Output intensities of the drilling process for the MPD system.

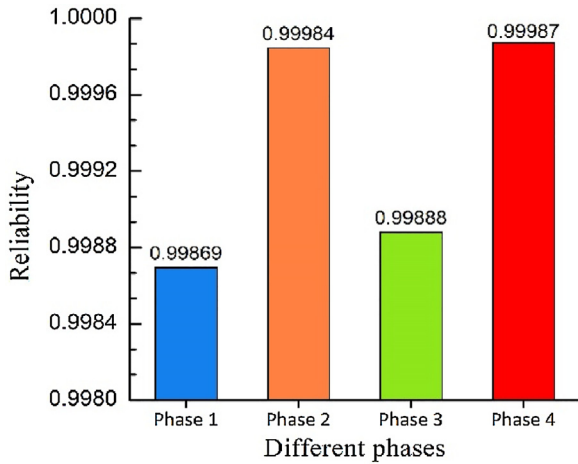


Fig. 12. Reliability of the drilling process for the MPD system.

S.112 is lower than operator S.112 due to the dependency among the causation factors. Output intensities of operator S.125 and S.127 are similar. As the endpoint of the drilling process for the MPD system, the output intensity of operator S.127 can also represent the reliability of the drilling process. Using this method, the reliability of four different phases (drilling process, making a connection, tripping out, and tripping in) are presented in Fig. 12. The reliability of “tripping in” and “making a connection operation” is higher compared to that of the drilling process and tripping out, while the “drilling process” is the lowest. The results indicate that the critical causes should be emphasized in the drilling process and the tripping out phases. For instance, the standby NRV can be installed or the speed of tripping out should be controlled to improve the reliability of the MPD system.

The change of dynamic reliability with depth is analyzed by DBN, as shown in Fig. 13. It is clear that the reliability of the MPD system decreases with increasing drilling depth. That is because the MPD system components will suffer some wear and tear with the drilling operation. The reliability of the descending slope is stable in

four respective drilling sections. The reliabilities go into a dramatic decline in different junctions between different sections. It is due to a job conversion, which decreases system reliability. The reliability of the MPD system decreases to 0.9348 when the 8–1/2 section is completed. As expected, when the MPD system works a long cycle in the deepwater drilling, the system reliability decreased significantly. Therefore, it is necessary to implement some maintenance to improve the system reliability by the decision-maker.

5.2. Sensitivity analysis and updating

It is evident that some components in a system are more important than any other. The sensitivity analysis is an effective method to identify the most critical component by changing the parameters of different components. In this study, the sensitivity of selected components was carried out at a certain phase instead of the entire drilling cycle. For example, the failure probability of the normal start ( $P_g$ ) for rig pump (RP) is changed to calculate the system reliability of the drilling process. Similarly, five different components are selected in different phases for the sensitivity analysis, and the results are shown in Fig. 14.

The steepness of the slope represents the sensitivity of components. The higher the steepness is, the more sensitive the component is. The sensitivity also illustrates the importance and criticality of different components in the system. As shown in Fig. 14(a), the sensitivity of the rig pump (RP) is higher than any other component, which indicates that the rig pump is the most crucial factor in the drilling phase. The drilling process would be forced to shut down once the rig pump fails. From Fig. 14, some conclusions can be deduced that rig pump (RP), check valve 1, RCD, and RP are the most sensitive components among selected components for different phases. And the sensitivity of the same component in different phases is unequal. For instance, RCD is the most sensitive component in tripping out, while in other phases, it is the least responsive element. Explanations for it is that the same component plays different roles in different phases due to the principles of operation and structural positions.

Another advantage of reliability assessment using DBN is the capacity to update reliability in real-time. For instance, when a

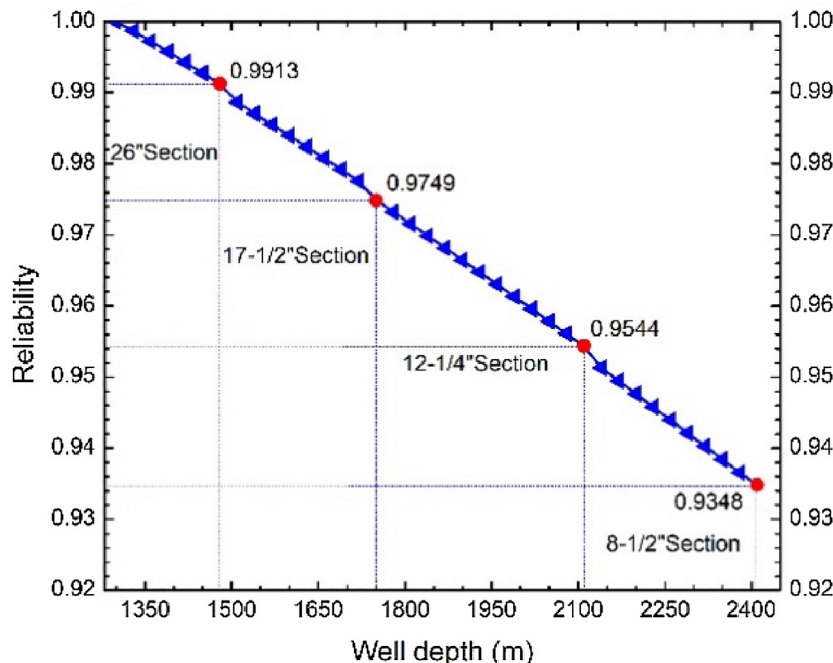


Fig. 13. Dynamic reliability of drilling cycle for the MPD system.

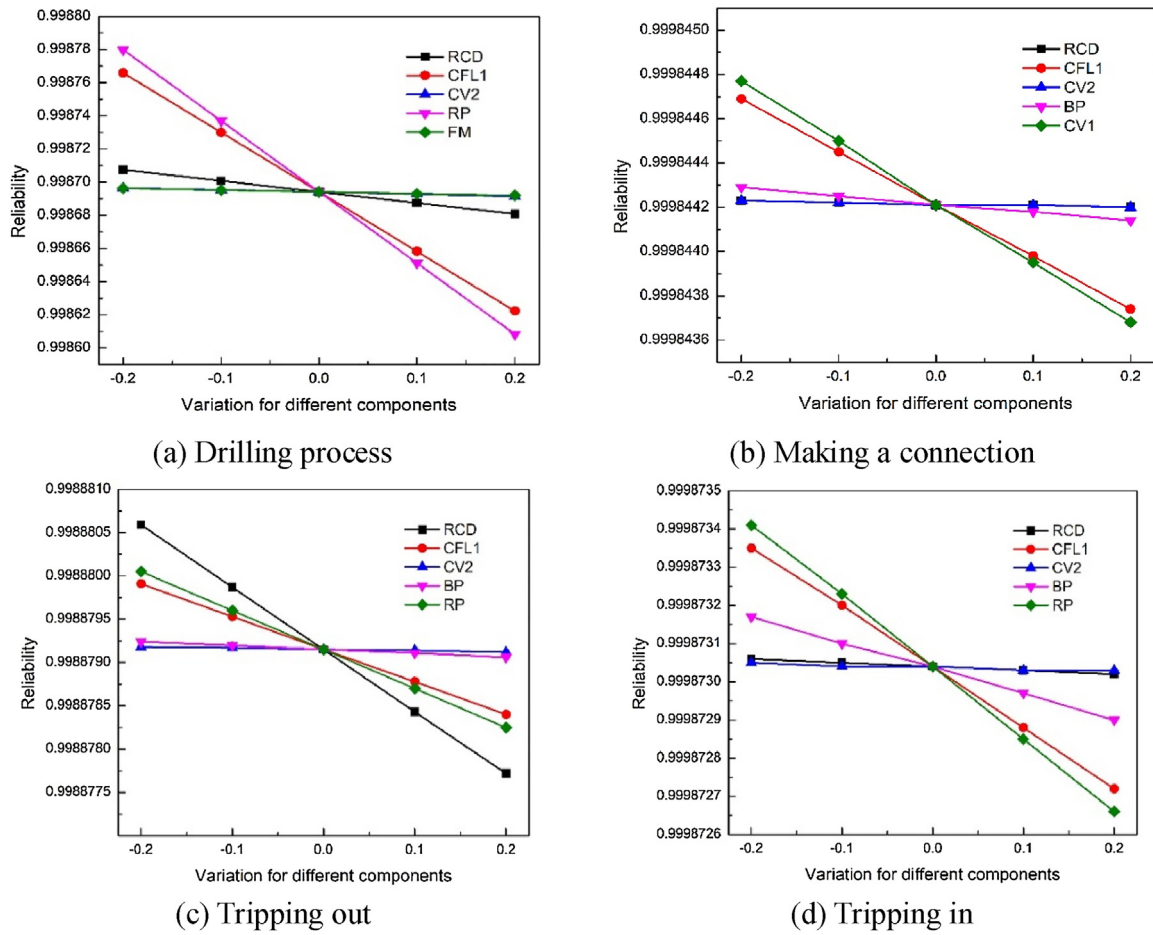


Fig. 14. Components important analysis of the MPD system for different phases.

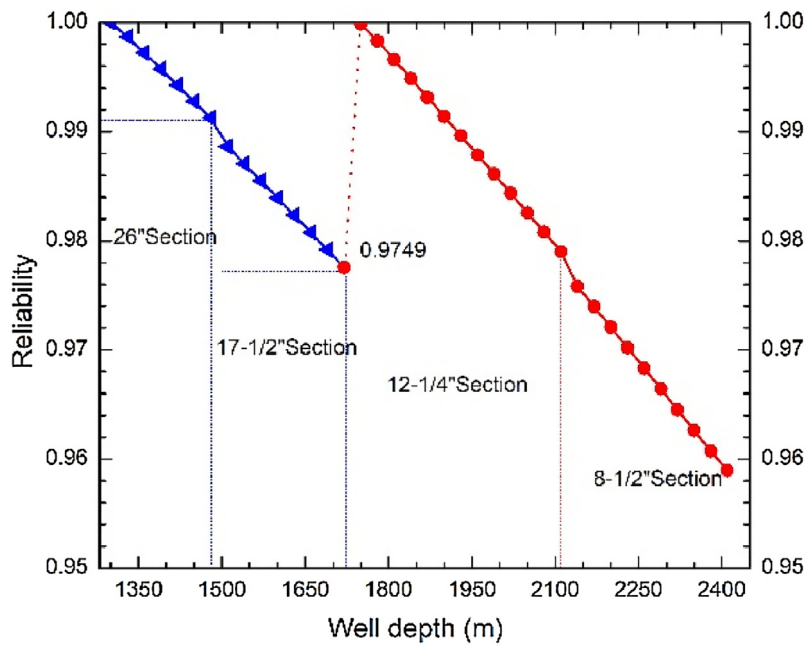


Fig. 15. Updated reliability of drilling cycle for the MPD system.

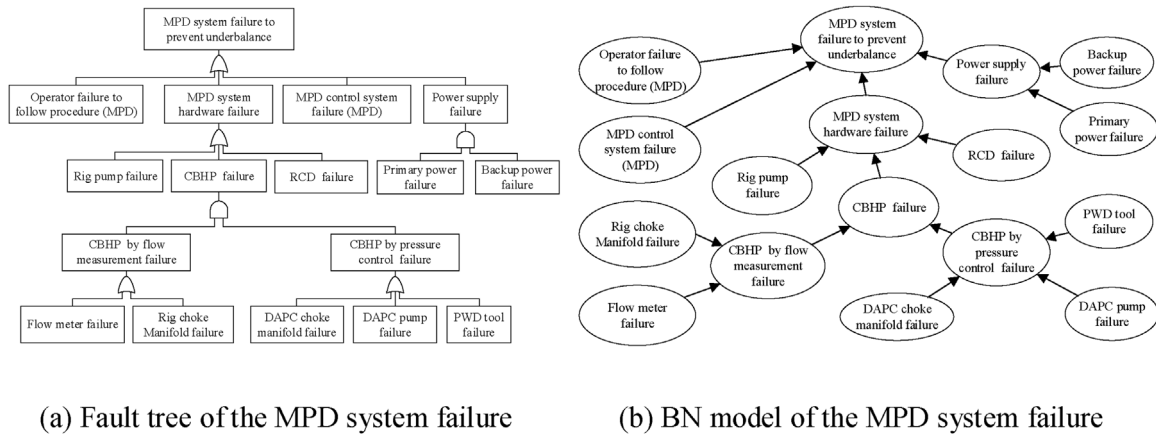


Fig. 16. Traditional models of MPD system failure.

new evidence  $E$  is given, the updated reliability of system  $Z$  can be calculated through  $R(Z | E)$ . The commonly used evidence in probability updating is the information about the specific consequence or event. In this paper, the MPD system typically works until drilling to 12–1/4" section, but the RCD needs to be replaced due to weariness. Otherwise, it may shut down as a result of sealing failure. Therefore, the new evidence is that a new RCD is changed when drilling to 1780 m. As shown in Fig. 15, the dynamic reliability of the MPD system can be updated and predicted in the remaining drilling operation based on this event. The reliability of the MPD system returns to 1 after replacing the RCD. Furthermore, the updated reliability decreases to 0.9589 when the drilling operation is completed. It can also capture some new observations simultaneously, and the dynamic reliability of the MPD system will be updated at different time points.

5.3. Validation of the model

Validation is a necessary and essential aspect of a proposed method as it will provide a reasonable amount of confidence to the results of the model and produce the required results in a sound and defensible manner (Jones et al., 2010). The validation of the developed model requires the monitoring records of its parameters. However, for the MPD system that we analyzed in this paper, these monitoring records are not available. Therefore, the validation in this particular study is conducted by a three-axioms-based sensitivity analysis method (Cai et al., 2013). The following three axioms must be satisfied: **Axiom 1**. A slight increase/decrease in the prior subjective probabilities of each parent node should certainly result in the effect of a relative increase/decrease of the posterior probabilities of the child node; **Axiom 2**. Given the variation of subjective probability distributions of each parent node, its influence magnitude to the child node values should keep consistency; **Axiom 3**. The total influence magnitudes of the combination of the probability variations from  $x$  attributes (evidence) on the values should always be greater than the one from the set of  $x$ - $y$  ( $y \in x$ ) attributes (sub-evidence).

The validation of the developed model aims to demonstrate the constructed model with rational analysis. The model should at least satisfy the three axioms described in Section 3.3. Taking the parent nodes of "S\_127" for example, the successful probability of a drilling process decreases from 99.87 % to 79.89 % when the failure probability of "S\_126" (Flow measurement) is set to 80 %. However, the successful probability decreases from 79.89 % to 49.93 % when the failure probability of "S\_126" is set to 50 %. When the "C\_127" (Mud Separator) of failure probability is set to 50 %, it results in a revised success probability of 49.94 % from 99.87 %. The result

indicates that the established model accords with Axiom 1 and 2. Furthermore, when both changes and the failure probabilities of the two nodes are set to 50 %, the successful probability decreases to 24.97 % from 99.87 %. The exercise of increasing failure probability of each influencing node satisfies the three axioms, thus giving a partial validation of the DBN model at its highest hierarchical level.

5.4. Method comparison

An early study was carried out to evaluate the safety and risk analysis of managed pressure drilling operations. In this study, a bow-tie model was developed to identify the root causes of kicks in an offshore drilling operation. In the bow-tie model, the kick event is the central event, culminating in a blowout and other escalated consequences. As a critical barrier to preventing the kick event, the fault tree (FT) model of the MPD system failure was developed, as shown in Fig. 16(a) (Abimbola et al., 2015). The obtained failure probability of the MPD system based on the FT model is  $1.0 \times 10^{-4}$ . However, the analytical results cannot be easily updated by the FT technique when new evidence or observations are given. The FT model for the MPD system is mapped into the BN model, as shown in Fig. 16(b). The posterior probability of the MPD system is updated to  $1.23 \times 10^{-3}$  by assuming a kick occurrence.

Compared with static BN, the proposed method is an integrated framework. The dynamic reliability of the MPD system can be obtained, considering the change of the environmental and operational conditions of the system. The reliability of the MPD system would be decreased from 99.98 % to 93.48 %, which means that the failure probability of the MPD system is  $2.0 \times 10^{-4}$ . It is of the same order of magnitude as that of Abimbola et al.,  $1.0 \times 10^{-4}$ , which can also validate the proposed method (Abimbola et al., 2015). The obtained dynamic and decreasing reliability of the MPD system matches the inherent property of the system. Furthermore, the proposed method produces a more rational result since the sequence operations, phased mission problems, and multiple processes of the MPD system are all considered.

6. Conclusions

This paper develops an integrated approach, which combines the GO-FLOW and DBN models for the dynamic reliability assessment of an MPD drilling operation considering the entire life cycle of a drilling process. The operation models of the MPD system are developed in different phases by using the GO-FLOW method because of its capacity to handle sequential operation and phased mission problems for complex systems. The corresponding DBN model for the MPD system is established to assess the dynamic reli-

ability throughout the entire drilling cycle. The DBN can also offer flexibility sensitivity analysis and information updating, which could be used to identify the critical components and update reliability.

The proposed method can be applied to assess system reliability considering a sequential operation, phased mission problem, and multiple processes. The dynamic reliability of the MPD system has been obtained during the entire drilling cycle. This method also assists in identifying the most sensitive components and achieving real-time reliability based on updated information. The case study demonstrates that the proposed method could be efficiently applied to the reliability assessment of the MPD system. In addition, this method can also be used for risk and reliability analysis of other offshore facilities and operations.

In this paper, the reliability assessment of the sequential operation system can be achieved by the proposed method. However, there are no uniform standards for the reliability level of the MPD system at present. The determination of the evaluation criteria may provide a directive function for the decision-makers to make the required decisions, so this will be part of our future work. On the other hand, the detailed maintenance strategies or decision-making should be constructed based on the reliability analysis results, which can improve the reliability of the MPD system.

### Declaration of Competing Interest

The authors declare that they have no known competing financial interests or personal relationships that could have appeared to influence the work reported in this paper.

### Acknowledgment

The authors gratefully acknowledge the financial support provided by National Key R&D Program of China (No: 2017YFC0804501), National Natural Science Foundation of China (No. 52004142) and Postgraduate Innovation Engineering Project of China University of Petroleum (East China) (No: YCX2020057). Author Faisal Khan thankfully acknowledges the financial support provided by Natural Science and Engineering Research Council of Canada (NSERC) and Canada Research Chair Program (Tier I) of Offshore Safety and Risk Engineering to strengthen the research collaboration.

### Appendix A

See Fig. A1 Tables A1–A3.

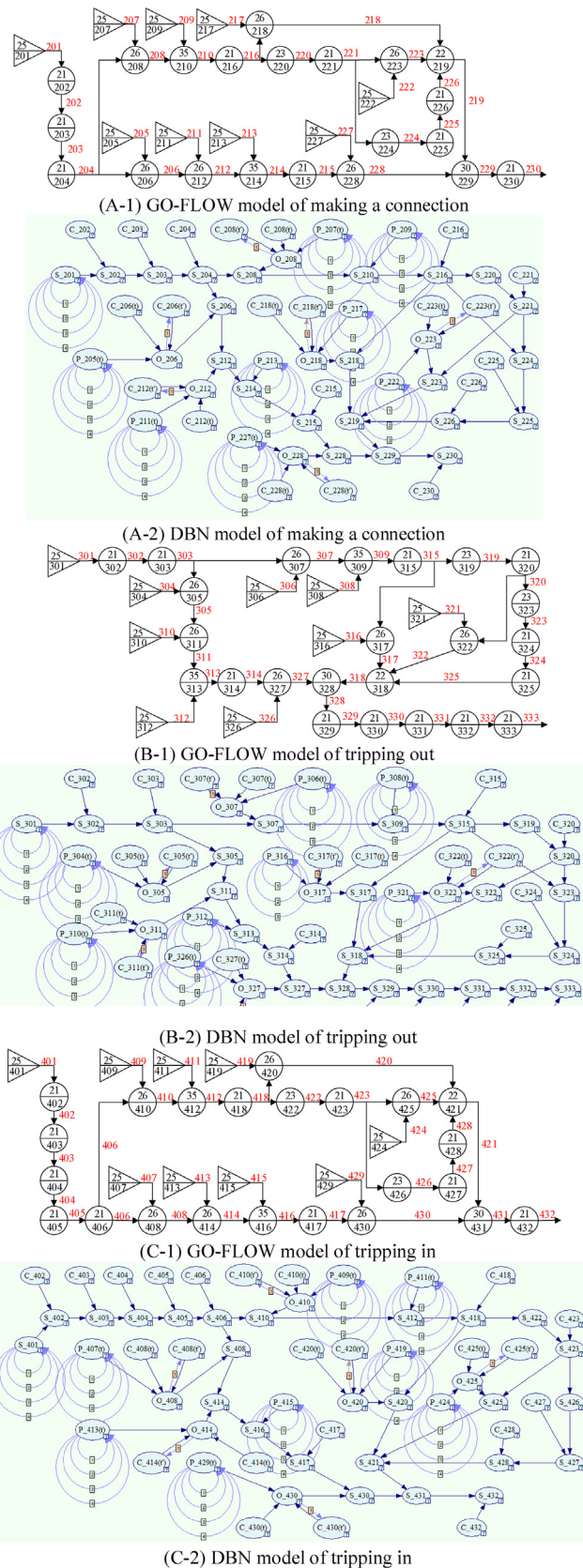


Fig. A1. GO-FLOW and DBN models of different phases for MPD system.

Appendix B

See Table B1.

**Table A1**  
The operator parameters of making a connection for MPD system.

Operator			Parameter	Operator			
No	Type	Meaning		No	Type	Meaning	
201	25	Initial time	$R(1) = 0 R(t) = 1 (t \neq 1)$	216	21	Choke flow line 1	$P = 3.6 \times 10^{-4}$
202	21	Stop top drive	$P = 3.0 \times 10^{-4}$	217	25	Start signal of choke valve 2	$R(t) = 0, t \neq (4,5) R(t) = 1, t=(4,5)$
203	21	Lifting	$P = 1.0 \times 10^{-4}$	218	26	Choke valve 2	$P_p = 2.5 \times 10^{-4} P_g = 2.5 \times 10^{-3}$
204	21	Adjust wellhead back pressure	$P = 1.0 \times 10^{-4}$	219	22	OR gate	/
205	25	Start signal of RCD	$R(2) = 1 R(t) = 0 (t \neq 2)$	220	23	NOT gate	/
206	26	RCD	$P_p = 6.7 \times 10^{-6} P_g = 6.7 \times 10^{-5}$	221	21	Choke flow line 2	$P = 3.6 \times 10^{-4}$
207	25	Start signal of rig pump	$R(3) = 1 R(t) = 0 (t \neq 2)$	222	25	Start signal of choke valve 3	$R(t) = 0, t \neq (4,5) R(t) = 1, t=(4,5)$
208	26	Rig pump	$P_p = 4.3 \times 10^{-5} P_g = 4.3 \times 10^{-4}$	223	26	Choke valve 3	$P_p = 2.5 \times 10^{-4} P_g = 2.5 \times 10^{-3}$
209	25	Time interval	$t = 0.1 \text{ h}$	224	23	NOT gate	/
210	35	Failure rate of rig pump	$\lambda = 2.52 \times 10^{-6} \text{ h}^{-1}$	225	21	Pressure relief valve	$P = 2.2 \times 10^{-5}$
211	25	Start signal of backpressure pump	$R(3) = 1 R(t) = 0 (t \neq 3)$	226	21	Backup flow line 3	$P = 3.6 \times 10^{-4}$
212	26	Backpressure pump	$P_p = 4.3 \times 10^{-5} P_g = 4.3 \times 10^{-4}$	227	25	Start signal of choke valve 1	$R(t) = 0, t \neq (4,5) R(t) = 1, t=(4,5)$
213	25	Time interval	$t = 0.1 \text{ h}$	228	26	Choke valve 1	$P_p = 2.5 \times 10^{-4} P_g = 2.5 \times 10^{-3}$
214	35	Failure rate of backpressure pump	$\lambda = 2.52 \times 10^{-6} \text{ h}^{-1}$	229	30	AND gate	/
215	21	Check valve 1	$P = 3.12 \times 10^{-3}$	230	21	Connect	$P = 1.5 \times 10^{-4}$

**Table A2**  
The operator parameters of tripping out for MPD system.

Operator			Parameter	Operator			
No	Type	Meaning		No	Type	Meaning	
301	25	Initial time	$R(1) = 0 R(t) = 1 (t \neq 1)$	318	22	OR gate	/
302	21	Start signal of tripping out system	$P = 1.0 \times 10^{-4}$	319	23	NOT gate	/
303	21	Adjust wellhead back pressure	$P = 1.0 \times 10^{-4}$	320	21	Choke flow line 2	$P = 3.6 \times 10^{-4}$
304	25	Start signal of RCD	$R(2) = 1, R(t) = 0 (t \neq 2)$	321	25	Start signal of choke valve 3	$R(t) = 0, t \neq (4,5) R(t) = 1, t=(4,5)$
305	26	RCD	$P_p = 6.7 \times 10^{-6} P_g = 6.7 \times 10^{-5}$	322	26	Choke valve 3	$P_p = 2.5 \times 10^{-4} P_g = 2.5 \times 10^{-3}$
306	25	Start signal of rig pump	$R(3) = 1 R(t) = 0 (t \neq 3)$	323	23	NOT gate	/
307	26	Rig pump	$P_p = 4.3 \times 10^{-5} P_g = 4.3 \times 10^{-4}$	324	21	Pressure relief valve	$P = 2.2 \times 10^{-5}$
308	25	Time interval	$t = 8 \text{ h}$	325	21	Backup flow line 3	$P = 3.6 \times 10^{-4}$
309	35	Failure rate of rig pump	$\lambda = 2.52 \times 10^{-6} \text{ h}^{-1}$	326	25	Start signal of choke valve 1	$R(t) = 0, t \neq (4,5) R(t) = 1, t=(4,5)$
310	25	Start signal of backpressure pump	$R(3) = 1 R(t) = 0 (t \neq 3)$	327	26	Choke valve 1	$P_p = 2.5 \times 10^{-4} P_g = 2.5 \times 10^{-3}$
311	26	Backpressure pump	$P_p = 4.3 \times 10^{-5} P_g = 4.3 \times 10^{-4}$	328	30	AND gate	/
312	25	Time interval	$t = 8 \text{ h}$	329	21	Pull out strings to certain depth	$P = 3.5 \times 10^{-4}$
313	35	Failure rate of backpressure pump	$\lambda = 2.52 \times 10^{-6} \text{ h}^{-1}$	330	21	Pump into weighted mud	$P = 1.0 \times 10^{-4}$
314	21	Check valve 1	$P = 3.12 \times 10^{-3}$	331	21	Continue to lift the drilling strings	$P = 3.0 \times 10^{-4}$
315	21	Choke flow line 1	$P = 3.6 \times 10^{-4}$	332	21	Close blind ram	$P = 2.6 \times 10^{-4}$
316	25	Start signal of choke valve 2	$R(t) = 0, t \neq (4,5) R(t) = 1, t=(4,5)$	333	21	Drilling tools change	$P = 1.0 \times 10^{-4}$
317	26	Choke valve 2	$P_p = 2.5 \times 10^{-4} P_g = 2.5 \times 10^{-3}$				

**Table A3**  
The operator parameters of tripping in for MPD system.

Operator			Parameter	Operator			
No	Type	Meaning		No	Type	Meaning	
401	25	Initial time	$R(1) = 0 R(t) = 1 (t \neq 1)$	417	21	Check valve 1	$P = 3.12 \times 10^{-3}$
402	21	Start signal of tripping in system	$P = 1.0 \times 10^{-4}$	418	21	Choke flow line 1	$P = 3.6 \times 10^{-4}$
403	21	Open blind ram	$P = 2.6 \times 10^{-4}$	419	25	Start signal of choke valve 2	$R(t) = 0, t \neq (4,5) R(t) = 1, t=(4,5)$
404	21	Running strings to certain depth	$P = 1.2 \times 10^{-4}$	420	26	Choke valve 2	$P_p = 2.5 \times 10^{-4} P_g = 2.5 \times 10^{-3}$
405	21	Replace weighted mud	$P = 1.0 \times 10^{-4}$	421	22	OR gate	/
406	21	Adjust wellhead back pressure	$P = 1.0 \times 10^{-4}$	422	23	NOT gate	/
407	25	Start signal of RCD	$R(2) = 1, R(t) = 0 (t \neq 2)$	423	21	Choke flow line 2	$P = 3.6 \times 10^{-4}$
408	26	RCD	$P_p = 6.7 \times 10^{-6} P_g = 6.7 \times 10^{-5}$	424	25	Start signal of choke valve 3	$R(t) = 0, t \neq (4,5) R(t) = 1, t=(4,5)$
409	25	Start signal of rig pump	$R(3) = 1, R(t) = 0 (t \neq 3)$	425	26	Choke valve 3	$P_p = 2.5 \times 10^{-4} P_g = 2.5 \times 10^{-3}$
410	26	Rig pump	$P_p = 4.3 \times 10^{-5} P_g = 4.3 \times 10^{-4}$	426	23	NOT gate	/
411	25	Time interval	$t = 8 \text{ h}$	427	21	Pressure relief valve	$P = 2.2 \times 10^{-5}$
412	35	Failure rate of rig pump	$\lambda = 2.52 \times 10^{-6} \text{ h}^{-1}$	428	21	Backup flow line 3	$P = 3.6 \times 10^{-4}$
413	25	Start signal of backpressure pump	$R(3) = 1, R(t) = 0 (t \neq 3)$	429	25	Start signal of choke valve 1	$R(t) = 0, t \neq (4,5) R(t) = 1, t=(4,5)$
414	26	Backpressure pump	$P_p = 4.3 \times 10^{-5} P_g = 4.3 \times 10^{-4}$	430	26	Choke valve 1	$P_p = 2.5 \times 10^{-4} P_g = 2.5 \times 10^{-3}$
415	25	Time interval	$t = 8 \text{ h}$	431	30	AND gate	/
416	35	Failure rate of backpressure pump	$\lambda = 2.52 \times 10^{-6} \text{ h}^{-1}$	432	21	Running drilling strings	$P = 1.2 \times 10^{-4}$



**Table B1**  
The specific parameters of well profile and work schedule in South China Sea.

No	Project	Content	Plan time (hour)	Total time (hour)	Phase time (day)	Depth (meter)
1	Mobilize	Navigate to well location	12	12	0.5	0
2	Predrilling preparation	Fixed position / Predrilling preparation	42	54	1.5	1200
3	36" section	Jetting operation	36	90	1.5	1300
4	26" section	Drilling 26" hole	24	114	1.75	1480
5		Cemented 20" casing	36	150	1.5	1480
6	Lower BOP	Lower BOP/pressure test	108	258	4.5	1480
7	17–1/2" section	Assembly 17 1/2" tools, drill plug, leak off test, drill 17 1/2" hole	54	312	2.25	1750
8		Cemented 16" casing	42	354	1.75	1750
9	12–1/4" section	Assembly 12–1/4" tools, drill plug, leak off test, drill 12–1/4" hole	60	414	2.5	2170
10		Electric logging	72	486	3	2170
11	8–1/2" section	Cemented 9–5/8" casing, BOP pressure test	60	546	2.5	2170
12		Assembly 8–1/2" tools, drill plug, leak off test, drill 8–1/2" hole	60	606	2.5	2440
13	Abandonment	Electric logging	60	726	2.5	2440
14		Plug and abandonment of offshore wells	168	894	7	2440
15	Demobilize	Platform demobilize	48	942	2	2440

## References

- Abimbola, M., Khan, F., Khakzad, N., 2014. Dynamic safety risk analysis of offshore drilling. *J. Loss Prev. Process Ind.* 30, 74–85.
- Abimbola, M., Khan, F., Khakzad, N., Butt, S., 2015. Safety and risk analysis of managed pressure drilling operation using Bayesian network. *Saf. Sci.* 76, 133–144.
- Amin, M.T., Khan, F., Imtiaz, S., 2018. Dynamic availability assessment of safety critical systems using a dynamic Bayesian network. *Reliab. Eng. Syst. Saf.* 178, 108–117.
- Arild, O., Ford, E.P., Loberg, T., Baringbing, J.W.T., 2009. *Kick Risk-A Well Specific Approach to The Quantification of Well Control Risks*. SPE, Jakarta, Indonesia, 124024.
- Bhandari, J., Abbassi, R., Garaniya, V., Khan, F., 2015. Risk analysis of deepwater drilling operations using Bayesian network. *J. Loss Prev. Process Ind.* 38, 11–23.
- Cai, B., Liu, Y., Liu, Z., Tian, X., Zhang, Y., Ji, R., 2013. Application of Bayesian networks in quantitative risk assessment of subsea blowout preventer operations. *Risk Anal.* 33, 293–311.
- Chang, Y., Wu, X., Zhang, C., Chen, G., Liu, X., Li, J., Cai, B., Xu, L., 2019. Dynamic Bayesian networks based approach for risk analysis of subsea wellhead fatigue failure during service life. *Reliab. Eng. Syst. Saf.* 188, 454–462.
- Chustz, M.J., Smith, L.D., Dell, D.M., 2008. *Managed Pressure Drilling Success Continues on Auger TLP*. SPE, Florida, USA, 112662.
- Fan, D., Wang, Z., Liu, L., Ren, Y., 2016. A modified GO-FLOW methodology with common cause failure based on discrete time Bayesian network. *Nucl. Eng. Des.* 305, 476–488.
- Gabaldon, O., Cullen, M., Brand, P., 2014. *Enhancing Well Control Through Managed Pressure Drilling*. OTC, Texas, USA, 25256.
- Hannegan, D.M., 2006. *Case Studies-Offshore Managed Pressure Drilling*. SPE, Texas, USA, 101855.
- Hashim, M., Yoshikawa, H., Matsuoka, T., Yang, M., 2013. Common cause failure analysis of PWR containment spray system by GO-FLOW methodology. *Nucl. Eng. Des.* 262, 350–357.
- Hashim, M., Hidekazu, Y., Takeshi, M., Ming, Y., 2014. Application case study of AP1000 automatic depressurization system (ADS) for reliability evaluation by GO-FLOW methodology. *Nucl. Eng. Des.* 278, 209–221.
- He, R., Li, X., Chen, G., Wang, Y., Jiang, S., Zhi, C., 2018. A quantitative risk analysis model considering uncertain information. *Process. Saf. Environ. Prot.* 118, 361–370.
- Jia, L., Lin, S., 2015. Current status and prospect for the methods of system reliability. *Syst. Eng. Electron.* 37 (12), 2887–2893.
- Jones, B., Jenkinson, I., Yang, Z., Wang, J., 2010. The use of Bayesian network modelling for maintenance planning in a manufacturing industry. *Reliab. Eng. Syst. Saf.* 95 (3), 267–277.
- Khakzad, N., Khan, F., Amyotte, P., 2013a. Dynamic safety analysis of process systems by mapping bow-tie into Bayesian network. *Process. Saf. Environ. Prot.* 91 (1–2), 46–53.
- Khakzad, N., Khan, F., Amyotte, P., 2013b. Quantitative risk analysis of offshore drilling operations: a Bayesian approach. *Saf. Sci.* 57, 108–117.
- Kim, H., Lee, H., Lee, K., 2005. The design and analysis of AVTMR (all voting triple modular redundancy) and dual-duplex system. *Reliab. Eng. Syst. Saf.* 88 (3), 291–300.
- Lan, X., Duan, F., Sang, Y., 2017. Application of GO-FLOW methodology in reliability analysis of aircraft EHA. *J. Beijing Univ. Aeronaut. Astronaut.* 43 (6), 1264–1270, 25.
- Li, X., Chen, G., Zhu, H., 2016. Quantitative risk analysis on leakage failure of submarine oil and gas pipelines using Bayesian network. *Process. Saf. Environ. Prot.* 103, 163–173.
- Li, X., Chen, G., Khan, F., Xu, C., 2019. Dynamic risk assessment of subsea pipelines leak using precursor data. *Ocean. Eng.* 178, 156–169.
- Liu, Z., Liu, Y., Wu, X., Yang, D., Cai, B., Zheng, C., 2016. Reliability evaluation of auxiliary feedwater system by mapping GO-FLOW models into Bayesian networks. *ISA Trans.* 64, 174–183.
- Liu, Z., Liu, Y., Wu, X., Cai, B., 2018. Risk analysis of subsea blowout preventer by mapping GO models into Bayesian networks. *J. Loss Prev. Process Ind.* 52, 54–65.
- Lu, H., Yang, M., Dai, X., Li, W., Yang, J., 2019. Reliability modeling by extended GO-FLOW methodology for automatic control component and system at NPP. *Nucl. Eng. Des.* 342, 264–275.
- Matsuoka, T., Kobayashi, M., 1988. GO-FLOW: a new reliability analysis methodology. *Nucl. Sci. Eng.* 98 (1), 64–78.
- Matsuoka, T., Kobayashi, M., 1989. GO-FLOW methodology: a reliability analysis of the emergency core cooling system of a marine reactor under accident conditions. *Nucl. Technol.* 84, 285–295.
- Matsuoka, T., Kobayashi, M., 1997. The GO-FLOW reliability analysis methodology-analysis of common cause failures with uncertainty. *Nucl. Eng. Des.* 175 (3), 205–214.
- Murphy, K.P., Ph.D. Thesis 2002. *Dynamic Bayesian Networks: Representation, Inference and Learning*, pp. 1–281.
- OREDA, 2002. *Offshore Reliability Data Handbook*, 4th ed, Distributed by Det Norske Veritas, P.O. Box 300, N-1322 Høvik, Norway.
- Pearl, J., 1988. *Probabilistic Reasoning in Intelligent Systems: Networks of Plausible Inference*. Morgan Kaufmann, San Francisco, California.
- Pui, G., Bhandari, J., Arzaghi, E., Abbassi, R., Garaniya, V., 2017. Risk-based maintenance of offshore managed pressure drilling (MPD) operation. *J. Pet. Sci. Eng.* 159, 513–521.
- Quoc, B., Yong, T., Singh, H.K.D., Nguyen, V.P., 2016. A Well Control Approach With Managed Pressure Drilling MPD on HPHT Wells in Vietnam-case History. SPE, Singapore, 180628.
- Rathnayaka, S., Khan, F., Amayotte, P., 2013. Accident modeling and risk assessment framework for safety critical decision-making: application to deepwater drilling operation. *Proc. Inst. Mech. Eng. Part O J. Risk Reliab.* 227 (1), 86–105.
- Shen, Z., Wang, Y., Huang, X., 2003. A quantification algorithm for a repairable system in the GO methodology. *Reliab. Eng. Syst. Saf.* 80 (3), 293–298.
- Sule, I., Khan, F., Butt, S., Yang, M., 2018. Kick control reliability analysis of managed pressure drilling operation. *J. Loss Prev. Process Ind.* 52, 7–20.
- Trucco, P., Cagno, E., Ruggeri, F., Grande, O., 2008. A Bayesian belief network modelling of organizational factors in risk analysis: a case study in maritime transport. *Reliab. Eng. Syst. Saf.* 93, 823–834.
- Veeramany, A., Pandey, M.D., 2011. Reliability analysis of nuclear component cooling water system using semi-Markov process model. *Nucl. Eng. Des.* 241 (5), 1799–1806.
- Wang, G., Fan, H., Liu, G., 2011. Design and calculation of a MPD model with constant bottom hole pressure. *Pet. Explor. Dev.* 38 (1), 103–108.
- Wu, S., Zhang, L., Fan, J., Zhou, Y., 2019. Dynamic risk analysis of hydrogen sulfide leakage for offshore natural gas wells in MPD phases. *Process. Saf. Environ. Prot.* 122, 339–351.
- Xu, K., Tang, L.C., Xie, M., Ho, S.L., Zhu, M.L., 2002. Fuzzy assessment of FMEA for engine systems. *Reliab. Eng. Syst. Saf.* 75 (1), 17–29.
- Yang, J., Yang, M., Yoshikawa, H., Yang, F., 2014. Development of a risk monitoring system for nuclear power plants based on GO-FLOW methodology. *Nucl. Eng. Des.* 278, 255–267.

- Yang, J., Wang, M., Guo, D., Zhang, B., Yang, M., 2020. Use of a success-oriented GO-FLOW method for system configuration risk management at NPPs. *Ann. Nucl. Energy* 143, 107452.
- Zhang, G., Thai, V.V., 2016. Expert elicitation and Bayesian network modeling for shipping accidents: a literature review. *Saf. Sci.* 87, 53–62.
- Zhang, L., Wu, S., Zheng, W., Fan, J., 2018. A dynamic and quantitative risk assessment method with uncertainties for offshore managed pressure drilling phases. *Saf. Sci.* 104, 39–54.
- Zhu, J., Collette, M., 2015. A dynamic discretization method for reliability inference in Dynamic Bayesian Networks. *Reliab. Eng. Syst. Saf.* 138, 242–252.